Advance Physics Letter

Investigation of electrochemical capacitance of core-shell structured poly (m-Aminophenol) (PmAP)/MoO_3 composite

[1]Muktikanta Panigrahi, [2]Benorita Prusty and [3]Munesh Chandra Adhikary
[1]Metallurgical Engineering Dept., Gandhi Institute of Engineering and Technology, Gunupur- 765022, Odisha, INDIA
[2,3]P.G. Department of Applied Physics and Ballistics, Fakir Mohan University, Balasore, Odisha, India
Email : muktikanta2@gmail.com

Abstract : Core-shell structure of PmAP/MoO_3 composite is successfully synthesized by chemical oxidative polymerization method. The synthesized composite is characterized by X-ray diffraction, FTIR, UV Visible, FESEM and cyclic-voltagram (CV) techniques. X-ray diffraction pattern of prepared composite is indicated the formation of intercalation. PmAP, MoO_3, and PmAP/MoO_3 composite are endorsed by FTIR spectral analyses. Mo-O stretching, benzene stretching, C=N, O-H stretching and C-H stretching are observed in FTIR spectra. Small crystal and aggregated small crystal are observed for PmAP and PmAP/MoO_3, respectively from morphological study. π-π* transition and charge transfer of polaron band of PmAP and PmAP/MoO_3 composite are found in UV Visible spectra, respectively. The optical band gap is found to be 3.09 eV. The Cyclic voltammetry analysis reveals the oxidation-reduction of poly (m-Aminophenol).

Key words: Core-shell structure, Intercalation, Morphology, Electrochemistry

I. INTRODUCTION

Polyaniline (PANI) is unique in conducting polymeric materials because of its easy synthesis, cheap, environmental stability, and wide applicability in electronic and optoelectronic areas but it shows poor processability [1-4]. Effort has been continuing for improving processability. One way of improving processability through chemical and electrochemical polymerization processes is modification of anilinic monomer such as substituted anilinic monomer [1-4]. Various substituted groups such as $–OCH_3$ [1], $-CH_3$ [2], $-SO_3H$ [3], -Cl, -F, -I [4], etc. of aniline at ortho and meta positions are reported. Generally, ortho-isomer is more preferred because the polymer synthesis gives better yield, higher conductivity [1-4] than that of meta-isomer. Aniline substituted polymer possesses lower conductivity than polyaniline due to the steric hindrance between the substituents [1-4]. Therefore, ladder structure is formed and shows poor solution processability along with conductivity.

Now a day, composite materials based on conducting polymers with transition metal oxides have become a popular basic material for potential application, such as active components in electrode material in lithium batteries [5]. Furthermore, they possess advanced properties via the modification of each other [6,7].

The synthesis of composites of core/shell inorganic nanoparticle/polymer has attracted much research attention in recent years because the core/shell nanocomposites might exhibit dual physical properties of core and shell materials [8–10]. In particular, the nanocomposites of core/shell metal oxide nanoparticles/conducting polymer (c/s-MO/polymer) combine the electrical properties of the polymer shell and the magnetic, optical, electrical or catalytic characteristics of the metal oxide core, which could greatly widen their applicability in the fields of catalysis, electronics and optics [8-10]. Many efforts have been made to successfully prepare nanocomposites such as c/s-SnO_2, −SiO_2, −CeO_2 or −Fe_2O_3/polypyrrole by chemical preparation and electrochemical method [11–14].

However, the desired properties of poly (m-aminophenol) are not satisfactory. In this regards, PmAP/MoO_3 composite may open way to construct novel organic-inorganic hybrid system showing ionic conductivity as well as good thermal properties.

It is known that molybdenum trioxide (MoO_3) is a typical host for many monovalent and multivalent cations inserted chemically or electrochemically. The insertion suitability of MoO_3 is due to its layered crystal structure. Edge- and corner- sharing [MoO_6] octahedra build up double layers, and these layer planes characterized by strong covalent bonds are held together by weak van der Waals attraction forces. Objective ions such as Li+ easily go into interlayers. The layered structure can be kept during the process of intercalation/deintercalation of lithium ion [15-17]. MoO_3 has been found to be very sensitive to various gases such as NO, NO_2, C_2H_5OH, CO, $H_2$and NH_3 in temperature range of 300–600 °C [18–22].

In the present work, we reported the synthesis of core shell structure of composite materials i.e., PmAP/MoO_3 composite with study of surface morphology, XRD, UV Visible, optical band gap, FTIR and Cyclic voltammeter

characterizations of pristine PmAP and PmAP/MoO_3 composite. The results are explained.

II. EXPERIMENTAL DETAILS

2.1. Materials

Synthesis grade of m-aminophenol (mAP) (Loba chemicals Pvt. Ltd., India), MoO_3 (Fluke, Switzerland), Ammonium perdisulphate (APS) (Merck, India), hydrochloric acid (HCl) (Merck, India), Dimethyl sulphoxide (DMSO), (Merck India) are purchased for synthesis of PmAP and PmAP/MoO3 composites. Deionised water was used for synthesis and washing purpose.

2.2. Synthesis of PmAP

PmAP was synthesized by chemically oxidative polymerization method using mAP as monomer and APS as oxidant. Mole ratio of mAP and APS was 1:1.5. The polymerization was done in a 3-necked round bottom flask [23]. Out of 3-necked flask, one neck was used for inserted thermometer to measure the reaction temperature, second neck was connected to the condenser to cool down the reaction temperature, and third neck was for drop wise addition of APS solution to the monomer solution. For the polymerization, two type of solution was required. **In solution-1**, 3.27 g of mAP (0.03 moles) and 50 mL of 1.8 M HCl solution was taken for the preparation of mAP solution. **In solution-2**, 10.26 g APS (0.045 moles) and 25 mL distilled water was used to prepare the APS solution. The reaction temperature was maintained at 80 °C. **Solution-2** was added drop wise on **solution-1** through injection syringe (45 min) and stirred 14-15 h. The brown colored precipitate was formed and it was stayed overnight after over the reaction. The precipitate was filtered and washed with 4 M HCl for 2-3 times for removing the traces of unreacted monomers and oligomers followed by washing with deionized water for several times till the filtrates becomes colorless from light brown color. Finally, prepared deep brown colored precipitates were dried in an oven at 70 °C for 10 h and collected the dried samples.

2.3. Synthesis of PmAP/MoO_3 composite (Core-shell)

Also, Core-shell structured PmAP/MoO_3 composite was synthesized by chemical oxidative polymerization technique in acid medium [11]. Mole ratio of mAP and APS was 1:1.5. For the polymerization process, two types of solution are needed. In **Solution A** contained 3.27 g mAP (0.03 moles) and 50 mL aqueous HCl (1.8 M). S**olution B** contained 10.26 g (0.045 moles) of APS and minimum volume of water (25 mL), called oxidant solution. Three nacked round bottom flask (**RB**) was used as reaction vessel. Centigrade thermometer was inserted through in one nack to measure the reaction temperature, second one was connected to the condenser, and third neck was used as addition of solution B to the solution A. Then, MoO_3 particle of 10 wt% was added to the monomer solution and stirred upto 1 h. Then, **solution B** was added drop wise through dropping funnel (45 min) to the **solution A.** The reaction temperature was maintained at 80 °C and stirred 14-15 h. The brown colored precipitate was formed and kept overnight. The precipitate was filtered and washed with 4 M HCl for 2-3 times for removing the traces of unreacted monomers and oligomers followed by washing with deionised water for several times till the filtrates becomes colorless. Finally, deep brown colored product was dried at 70 °C in an oven for 10 h and collected the dried product.

2.4. Pellets Preparation

Pellets for measuring the electrical conductivity were prepared by compression molding with pelletizer. A pressure of 124 MPa was applied for five min to form pellet. Removing the pressure from the compression molding, pelletizer is removed. After that, the pellet was removed. Thicknesses and diameter of pellets were found to be 1.10 mm and 15.76 mm, 1.09 mm and 15.76 mm, respectively.

III. INSTRUMENTATION

WXRD experiments were performed using a Phillips PW-1710 Advance wide-angle X-ray diffractometer and Phillips PW-1729 X-ray generator with CuKα radiation (wavelength, $\lambda = 0.154$ nm). The generator was operated at 40 kV and 20 mA. The powder samples were placed on a quartz sample holder at room temperature and were scanned at diffraction angle 2θ from 5° to 60° at the scanning rate of 2°/ min. **FTIR s**pectra were recorded on a Thermo Nicolt Nexus 870 spectrophotometer in the range 400-4000 cm^{-1}. The instrument settings were kept constant (50 scan at 4 cm^{-1} resolution, Absorbance measurement mode). Pellets were prepared by compression molding using a pelletizer and potassium Bromide (KBr). Before running the samples, a background spectrum was collected. Then samples were put in a sample holder and data were collected. For **UV-Visible spectra analysis,** the samples were dissolved in dimethyl sulphoxide (DMSO). The UV-Visible spectra of the pristine polyaniline its nanocomposites were recorded by using a Micropack UV-VIS-NIR, DH 2000 in the wave length region 200-1000cm^{-1}. Base line was corrected before recording the spectra. surface morphologies of the neat polymer and its composite were analyzed by field emission scanning electron microscopy (**FESEM**). FESEM measurements were performed in Carl Zeiss Supra 40 scanning electron microscope. Powder samples were used with gold coating before FESEM measurements. Samples were operated at a voltage 4 kV. **An Auto lab PGSTAT302 potentiostat/galvanostat** was employed to perform CV measurements in the different pH solutions: pH (0.5 M $HClO_4$).

IV. RESULTS AND DISCUSSION

4.1. XRD analysis

XRD analysis is used for determining the degree of intercalation of MoO_3 in the polymer matrix. **Fig.** 1

shows the XRD patterns of pure MoO_3 (**A**) and PmAP/MoO_3 composite (**B**). PmAP/MoO_3 composite shows discernible peak in the XRD patterns, indicating that the positions of the characteristic peaks of the two products are not consistent and shifted to lower angle, must of MoO_3 layers are intercalated in the polymer matrix [24]. All the diffraction peaks of MoO_3 can be indexed to the pure phase of MoO_3 with the orthorhombic structure, indicating that the products are of high purity [25].

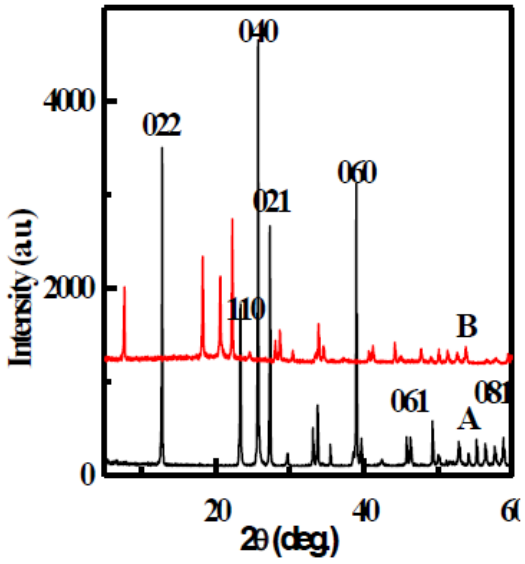

Figure 1 XRD patterns of MoO3 (A) and PmAP/ MoO3 composite (B)

4.2. FTIR analysis

The most important task for successful conversion analysis by FTIR is selection of the peaks employed in the analysis for neat PmAP and PmAP/MoO_3. FTIR spectrum of MoO_3 particle is shown in the **Fig. 2**(A). It indicates two different bands at 550-600 cm^{-1} and 950-1000 cm^{-1}, which corresponds to the presence of Mo-O and Mo=O bond [26], respectively. It is cleared from **Fig. 2 (A)** that the required group(s) is retained in MoO_3 materials.

Fig. 2(B) shows the spectrum of PmAP polymer. The peak position is found at 3360 cm^{-1}, which is assign to the presence of -OH group in the PmAP polymer. The -NH stretching band of is obtained at 3202 cm^{-1} in the spectrum. The imine i.e., -C=N- group bands appears at 1620 cm^{-1} due to the presence of in polymer. The peak at 2930 cm^{-1} shows the presence of -CH group in the polymer. The band at 1287 cm^{-1} is close to -C-O stretching band. This means most of the -OH groups remain free after polymerization. All the required groups are presented in the PmAP polymer [27].

Fig 2(C), the characteristics bands of PmAP/MoO_3 composite are found to be 3742, 3375, 3197, 2939, 1620, 1502, 1313, 986, 897 cm^{-1}, respectively. This peak shows the presence of both components i.e., pure PmAP and MoO_3 in the PmAP/MoO_3 (10 wt %) composite. We observed that some bands of PmAP to relatively high frequency with sharp intense peaks due to the presence of MoO_3 in the composite as shown in the **Fig 2**(C). Thus, formation of PmAP and their subsequent incorporation i.e., MoO_3 in the PmAP/MoO_3 and composite was endorsed by **FTIR** spectral analyses.

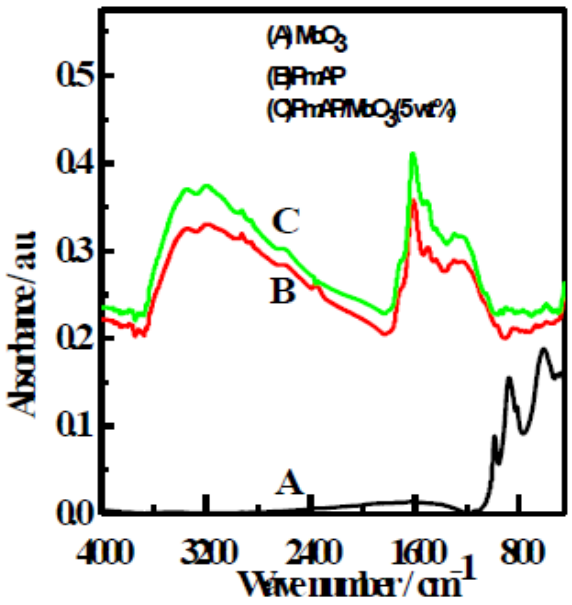

Figure 2 FTIR spectra of MoO3 particles (A), PmAP (B) and PmAP/MoO3 composite (C)

4.3. UV Visible analysis

UV Visible spectra of PmAP and PmAP/MoO_3 are presented in the **Fig. 3**. It is clear from that **Fig. 3** that PmAP has characteristic peaks at 322 nm corresponds to π-π^* transition of the benzenoid ring and 514 nm peak for electronic excitation from Benzenoid ring to Quinoid ring [26,27]. The shifting of bands from 514 nm to 518 nm i.e., higher wavelength indicates an increase of conjugation length, a decrease of band gap energy, and a delocalization of electrons in the electronic excitation band from neat polymer to composite polymer. The band area of composite is higher than the neat polymer. This shows that more conjugation occurs in composite material.

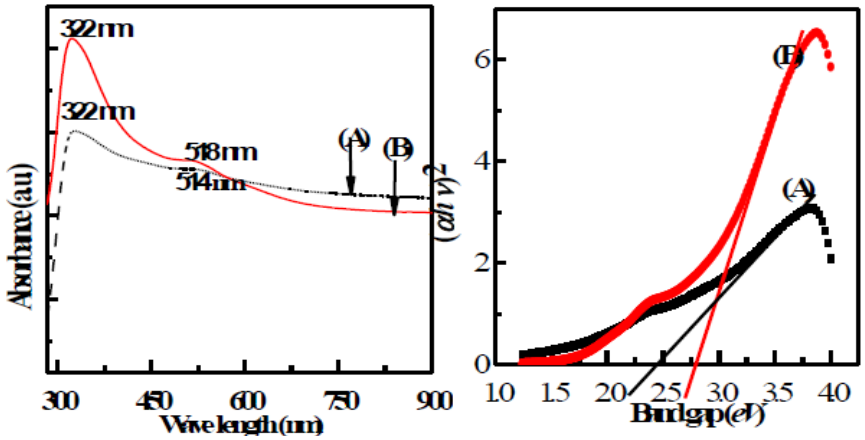

Figure 3 UV Visible spectra (left side Fig 3) of pure PmAP and PmAP/MoO3 composite Band gap (right side Fig.3) of PmAP polymer and PmAP/MoO3 composites

The energy band gap of the as-prepared polymer and its composites has been calculated with the help of absorption spectra. To calculate the optical band gap energy from absorption spectra using the Tauc expression [28] is

$$\alpha h\nu = A\,[h\nu - E_g]^n \text{ ----------(1)}$$

where **hν** is the photon energy, **h** is Planck's constant, **α** is the absorption coefficient, E_g is the optical energy gap, **A** is the constant, for direct transitions **n=1/2**. We plot a graph between $(\alpha h\nu)^2$ vs. hν, the extrapolation of the straight line to $(\alpha h\nu)^2 = 0$ axis gives E_g. **Fig.3 (right side)** shows the plots of $(\alpha h\nu)^2$ versus hν for the PmAP and PmAP/MoO_3, respectively. The values of E_g obtained for doped polypyrrole and polyaniline are 1.75 and 1.60 eV, respectively

4.4. FESEM analysis

Fig. 4 showed that FESEM images of PmAP and PmAP/MoO_3 (10 wt%) composite. The surface morphology of PmAP exhibits crystal-like structure and having the crystal size less than 1 µm. The prepared composite i.e, PmAP/MoO_3 (10 wt%) shows aggregated small crystal and having size more than 1 µm. This results showed that MoO_3 particles are strongly interacted the PmAP. In order to confirm the presence of Mo in the MoO_3 micro particles, EDX analysis was carried out. The quantitative analysis for EDX was performed only for C, N and Mo at different points. **Fig. 4** shows the EDX spectrum of MoO_3 micro particles in PmAP/MoO_3composite.

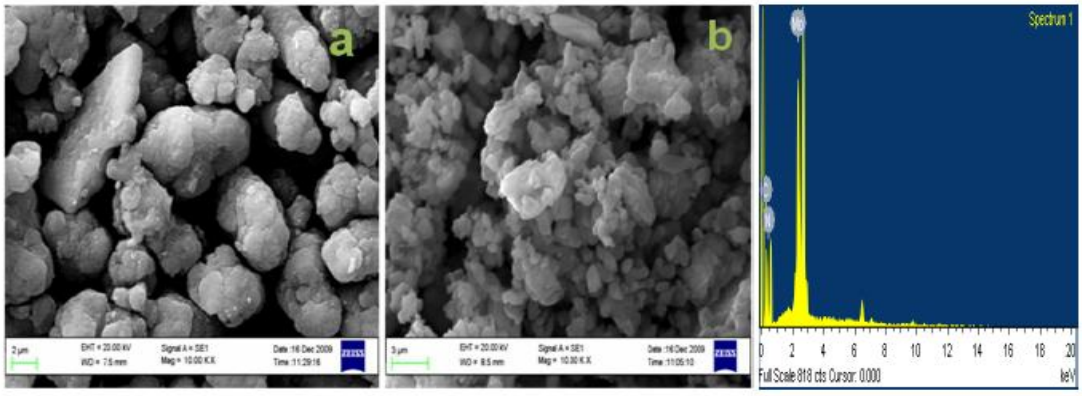

Figure 4 FESEM images of PmAP (a), PmAP/MoO3 (10 wt%) composite (b) and EDX analysis of PmAP/MoO3 composite

4.5. Electrochemical analysis

The Electrochemical measurements are performed in a three electrode arrangement system. The electrodes such as silver electrode for reference electrode, platinum electrode for counter electrode, and glassy carbon-electrodes for working electrode are used. Oxygen is removed from solution by bubbling nitrogen gas for 10 min and then a N_2 atmosphere is maintained during the measurements. Glassy carbon electrode (GCE) by using electrochemical procedures exhibit somewhat electrocapacitive effect towards the redox of some electro-active substances [29-32]. Therefore, prior to modification, GCE is usually pre-treated via chemical oxidation in strong acid medium, such as $HClO_4$. The ohmic potential drop is measured and is introduced in the Auto lab software. The measurements are performed between 0.2 and +0.7 V. The characterization by means of cyclic voltammetry (CV) has been done at one scan

rates as it has been corroborated the influence of this parameter on the electrochemical response obtained. The scan rates employed were 50 V s.

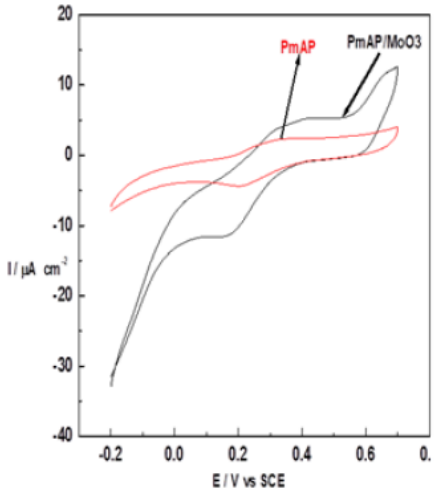

Figure 5 Voltammograms (CV) in the range -0.2 V and +0.7 V of PmAP and PmAP/MoO3 at 50 V/s

To determine the oxidation and reduction potentials for electrochemical performances such as capacitive behavior of PmAP and PmAP/MoO_3 composites, it is used a CV. The capacitance estimated from the CV curve is reported by integrating over the CV curve to determine the average value of the area for one cycle [33]. In PmAP loop, it shows an oxidation peak located at + 0.3 V and a reduction peak located at +0.25 V. Similarly, In PmAP/MoO_3 composites, it shows an oxidation peak located at + 0.4 V and a reduction peak located at +0.20 V.

As can be seen in **Fig. 5**, there are two peaks originating from the PmAP, and it exhibits a small-loop having low current density response. When compared with the PmAP, however, the current density response and the CV loop area of the and PmAP/MoO_3 composites is much higher, which clearly indicates that the electrochemical performance of the composites is remarkably enhanced owing to the presence of the MoO_3 particles inside the PmAP polymer. One pair of well-defined redox peaks appeared for the composites, which are attributed to one redox transitions of PmAP/MoO_3, also suggesting the presence of pseudocapacitive PmAP/MoO_3 [34]. The peaks correspond to the redox transitions between a semiconducting state (the leucoemeraldine form) and a conducting state (polaronic emeraldine) designated as peaks **C1/A1**, and the Faradaic transformation of emeraldine to pernigraniline initiates the redox peaks **C2/A2** [30]. From the CVs recorded for the PmAP and PmAP/MoO_3 composite at 50V/s scan rates, it was noticed that the cathodic peaks shift positively and the anodic peaks shift negatively. It should be noted that the synergetic effect resulting from the interactions of PmAP and MoO_3 may affect the shape and potential position of the CV curves, as clearly evident from our results. As exhibited in **Fig. 5**, the CV curve of the PmAP and PmAP/MoO_3 is close to being rectangular shaped, which might indicate that it possesses excellent electrical double-layer capacitance.

V. CONCLUSION

We have successfully synthesizes of poly (m-aminophenol) with MoO_3 by interfacial polymerization, wherein layered crystal structured of the MoO_3 were intercalated. The amount of MoO_3 content plays a vital role in controlling the structure of the composites and, hence, various materials properties. Optical studies of PmAP and PmAP/MoO_3 composites showed absorption peak for $\pi \rightarrow \pi^*$ transition and charge transfer spectra. The optical band gap is estimated using Tauc expression. Concerning the morphology of PmAP and PmAP/MoO_3, a globular-shaped topographic structure was obtained. The cyclic voltammetry results of PmAP/MoO_3 composites are shown better capacitance.

ACKNOWLEDGEMENT

The support and accomplishment of research work at Metallurgical Engineering Department of Gandhi Institute of Engineering and Technology (**GIET**) is gratefully acknowledged. We also acknowledge the use of lab facilities provided by PG Department of Applied Physics & Ballistics, F. M. University, Balasore for doing the research work. The support of characterization work at Central Research Facility (CRF) of Indian Institute of Technology (IIT), Kharagpur is gratefully acknowledged

REFERENCES

[1] F. Cataldo, P. Maltese, Synthesis of alkyl and N-alkyl-substituted polyaniline: A study on their spectral properties and thermal stability, European Polymer Journal 38 (2002) 1791-1803.

[2] A. Falcou, A. Dhcuene, P. Hourquebie, D. Marsaeq, A. Balland-Longeall, A new chemical polymerization process for substituted anilines: Application to the synthesis of poly(N-alkylanilines) and poly(o-alkylanilines) and comparison of their respective properties, Synthetic Metals 149 (2005) 115-122.

[3] Y.W. Park, J.S. Moon, M.K. Bak, J.-I. Jin, Electrical properties of polyaniline and substituted polyaniline derivatives, Synthetic Metals 29, (1989), 389-394.

[4] J. Yue, A.J. Epstein, Synthesis of self-doped conducting polyaniline, Journal of American Chemical Society 112 (1990) 2800-2801.

[5] V M Mohan, W Chen, K Murakami, Synthesis, structure and electrochemical properties of polyaniline/MoO_3 nanobelt composite for lithium battery, Materials Research Bulletin, 48, (2013) 603-608.

[6] N. Ballav, M. Biswas, Conductive composites of polyaniline and polypyrrole with MoO_3 Materials Letters, 60 (2006) 514-517.

[7] Y. Li, Y. Xiang, X. Dong, J. Xu, F. Ruan, Q. Pan, Polymerization of aniline in the interlayer space of molybdenum trioxide and its electrochemical properties, Journal of Solid State Chemistry 182 (2009) 2041-2045.

[8] T. Wen**,** Q. Fan**,** X. Tan**,** Y. Chen**,** C. Chen**,** A. Xu**,** X. Wang**,** A core-shell structure of polyaniline coated protonic titanate nanobelt composites for both Cr(VI) and humic acid removal, Polymer Chemistry 7 (2016) 785-794.

[9] M. H. Yang**,** S. B. Hong**,** B. G. Choi**,** Hierarchical core/shell structure of MnO_2/polyaniline composites grown on carbon fiber paper for application in pseudocapacitors, Physical Chemistry Chemical Physics 17 (2015) 29874-29879.

[10] C. Tian, Y. Du, P. Xu, R. Qiang, Y. Wang, D. Ding, J. Xue, J. Ma, H. Zhao, X. Han, Constructing Uniform Core-Shell PPy/PANI Composites with Tunable Shell Thickness toward Enhancement in Microwave Absorption, ACS Applied Materials Interfaces 7 (2015) 20090-20099.

[11] R. Liu , D. Li , C. Wang , N. Li, Q. Li, X. Lü, J. S. Spendelow, G. Wu, Core-shell structured hollow SnO_2-polypyrrole nanocomposite anodes with enhanced cyclic performance for lithium-ion batteries, Nano Energy 6 (2014) 73-81.

[12] J. Y. Wu, K. Y. Hsu, Controllable fabrication of SiO_2-polypyrrole core-shell dimer and trimer spheres, Journal of Materials Science: Materials in Electronics, 26 (2015) 3148-3154.

[13] X. Wang, T. Wang, D. Liu, J. Guo, and P. Liu, Synthesis and Electrochemical Performance of CeO_2/PPy Nanocomposites: Interfacial Effect, Industrial & Engineering Chemistry Research 55 (2016) 866-874.

[14] S. Xuan, Q. Fang, L. Hao, W. Jiang, X. Gong, Y. Hu, Z. Chen, Fabrication of spindle Fe_2O_3/polypyrrole core/shell particles by surface-modified hematite templating and conversion to spindle polypyrrole capsules and carbon capsules, Journal of Colloid and Interface Science 314 (2007) 502-509.

[15] M. T. Greiner, L. Chai, M. G. Helander, W.-M. Tang, Z.-H. Lu, Metal/Metal-Oxide Interfaces: How Metal Contacts Affect the Work Function and Band Structure of MoO_3, Advanced Functional Materials, 23 (2013) 215-226.

[16] M. Kröger, S. Hamwi, J. Meyer, T. Riedl, W. Kowalsky, Role of the deep-lying electronic states of MoO_3 in the enhancement of hole-injection in organic thin films, Applied Physics Letter 95 (2009) 123301-123303.

[17] T. Ressler, J. Wienold, R. E. Jentoft, F. Girgsdies, Evolution of Defects in the Bulk Structure of MoO_3 During the Catalytic Oxidation of Propene, European Journal of Inorganic Chemistry 2003 (2013) 301-312.

[18] M. Ferroni, V. Guidi, G. Martinelli, M. Sacerdoti, P. Nelli and G. Sberveglieri, MoO_3-based sputtered thin films for fast NO_2 detection, Sensors and Actuators B, 48 (1998) 285-288.

[19] K. Galatsis, Y. X. Li, W. Wlodarski, K. Kalantar-Zadeh, Sol-gel prepared MoO_3-WO_3 thin-films for O_2 gas sensing, Sensors and Actuators B: Chemical 77(2001) 478-483.

[20] K. Prasad, P. I. Gouma, D. J. Kubinski, J. H. Visser, R. E. Soltis and P. J. Schmitz, Reactively sputtered MoO_3 films for ammonia sensing, Thin Solid Films 436 (2003) 46-51.

[21] C. Imawan, H. Steffes, F. Solzbacher, E. Obermeier, A new preparation method for sputtered MoO_3 multilayers for the application in gas sensors, Sensors and Actuators B: Chemical 78 (2001)119-125.

[22] K. Galatsis, Y. X. Li, W. Wlodarski, E. Comini, G. Faglia, G. Sberveglieri, Semiconductor MoO_3-TiO_2 thin film gas sensors," Sensors and Actuators B: Chemical, 77 (2001) 472-477.

[23] P. Kar, N. C. Pradhan, B. Adhikari, A novel route for the synthesis of Processable conducting poly(m-aminophenol), Materials Chemistry and Physics, 111 (2008) 59-64.

[24] O. Yu. Posudievsky, S. A. Biskulova, V. D. Pokhodenko, New polyaniline–MoO_3 nanocomposite as a result of direct polymer intercalation, Journal of Materials Chemistry 12 (2002) 1446-1449.

[25] A. Kanneganti, C. Manasa, P. Doddapaneni, A Sustainable Approach Towards Synthesis of MoO_3 Nanoparticles using Citrus Limetta Pith Extract, International Journal of Engineering and Advanced Technology (IJEAT) 3 (2014) 128-130.

[26] A. Chithambararaj, D. B. Mathi, N. R. Yogamalar A. C. Bose, Structural evolution and phase transition of $[NH_4]_6Mo_7O_{24}.4H_2O$ to 2D layered MoO_{3-x}, Materials Research Express 2 (2015) 055004-055013.

[27] M. E. M. Hassouna, M.E.M.A. Hafez, Poly m-Aminophenol/Montmorillonite Nanocomposite for Adsorption of Lead from Authentic Water Samples and Spiked River Nile Water, International Journal of Engineering Research & General Science 3 (2015) 6-18.

[28] H. S. Abdulla, A. I. Abbo, Optical and Electrical Properties of Thin Films of Polyaniline and

Polypyrrole, International Journal of Electrochemical Science 7 (2012) 10666-10678.

[29] J. Molina, M. F. Esteves, J. Fernández, J. Bonastre, F. Cases, Polyaniline coated conducting fabrics. Chemical and electrochemical characterization, European Polymer Journal 47 (2011) 2003-2015.

[30] R. Ansari, M. B. Keivani, Polyaniline Conducting Electroactive Polymers: Thermal and Environmental Stability Studies, E-Journal of Chemistry 3 (2006) 202-217.

[31] L. Zhang, Q. Lang, Z. Shi, Electrochemical Synthesis of Three-Dimensional Polyaniline Network on 3-Aminobenzenesulfonic Acid Functionalized Glassy Carbon Electrode and Its Application, American Journal of Analytical Chemistry 1 (2010) 102-112.

[32] G. Zhang, X. Li , H. Jia, X. Pang, H. Yang, Y. Wang, K. Ding, Preparation and Characterization of Polyaniline (PANI) doped $Li_3V_2(PO_4)_3$, International Journal of Electrochemical Science 7 (2012) 830-843.

[33] Y. Wang, H. Xu, J. Zhang, G. Li, Review Electrochemical Sensors for Clinic Analysis, Sensors 8 (2008) 2043-2081.

[34] R. Ansari, Review Article Polypyrrole Conducting Electroactive Polymers: Synthesis and Stability Studies, E-Journal of Chemistry 3 (2006) 186-201.